Methylation Genome-Wide Profiling in Lowly and Highly Efficient Somatic Cell Nuclear Transfer in Pigs

Maciej Grzybek [1,*], Krzysztof Flisikowski [2], Tom Giles [3,4], Marta Dyjak [5], Rafal Ploski [6], Piotr Gasperowicz [6], Richard D. Emes [3,4] and Pawel Lisowski [7]

1. Department of Tropical Parasitology, Institute of Maritime and Tropical Medicine, Medical University of Gdansk, Powstania Styczniowego 9B, 81-429 Gdynia, Poland
2. Chair of Livestock Biotechnology, Technische Universität München, Liesel-Beckmann Str. 1, D-85354 Freising, Germany
3. School of Veterinary Medicine and Science, Sutton Bonington Campus, University of Nottingham, Leicestershire LE12 5RD, UK
4. Advanced Data Analysis Centre, University of Nottingham, Nottingham NG7 2RD, UK
5. Department of Animal Behavior, Institute of Genetics and Animal Breeding, Polish Academy of Sciences, Jastrzebiec, 36A Postepu Street, 05-552 Magdalenka, Poland
6. Department of Medical Genetics, Medical University of Warsaw, 3c Pawińskiego Street, 02-106 Warsaw, Poland
7. Department of Molecular Biology, Institute of Genetics and Animal Breeding, Polish Academy of Sciences, Jastrzebiec, 36A Postepu Street, 05-552 Magdalenka, Poland
* Correspondence: maciej.grzybek@gumed.edu.pl

Abstract: Swine is a common model organism for biomedical research. Epigenetic reprogramming in somatic cell nuclear transfer (SCNT) embryos does not fully recapitulate the natural DNA demethylation events at fertilisation. This study aimed to conduct genome-wide methylation profiling to detect differentially methylated regions (DMRs) responsible for epigenetic differences in stem cells that displayed high and low efficiency of SCNT and to elucidate the low efficiency of cloning rate in pigs. Adipose tissue mesenchymal stem cells (AMSC)s lines were isolated from adipose tissue of adult male pigs (n = 20; high-efficiency cells = 10; and low-efficiency cells = 10). Reduced representation bisulfite sequencing (RRBS) was performed on an Illumina HiSeq1500. Paired-end reads were filtered to remove the adapter contamination, and low-quality reads using TrimGalore! Filtered reads were mapped to the reference genome using Bismark. MethylKit was used to identify differentially methylated regions (DMRs) (bases and tiles), showing statistically significant differential methylation between high and low-efficiency AMSCs. Hierarchical cluster analysis according to methylation patterns clearly defined groups with low and high cloning efficiency. We report 3704 bases with statistically significant differences in methylation and 10062 tiles with statistically significant differences in methylation. Most differentially methylated sites are intergenic 62%, 31% are intronic, 4% are in exons, and 4% in promoters. Moreover, 37% of differentially methylated sites are located in known CpG islands (CGIs), and 4% in CpG island shores (CGSs).

Keywords: SCNT; RRBS; AMSC; DNA methylation; epigenetics; epigenomics; disease modeling; genetic engineering

1. Introduction

Animal-based disease modeling has become an interest in biomedical research, including cancer, metabolic, cardiovascular, and neurological disorders [1–5]. Swine has been an interest for basic and applied biomedical research for more than 20 years [6–8]. Swine plays an essential roles as a model of human diseases (Figure 1), including cardiovascular disease, cancer, diabetes, toxicology, and lipoprotein metabolism as a model organism [9–12]. The first generation of a pig using the somatic cell nuclear transfer (SCNT) method was conducted in 2000 [13–15], and since this time many genetically modified cloned pigs

have been generated [16–18]. Despite the success in generating of cloned individuals, there are still limitations that need to be improved to increase the efficiency of the porcine SCNT technique.
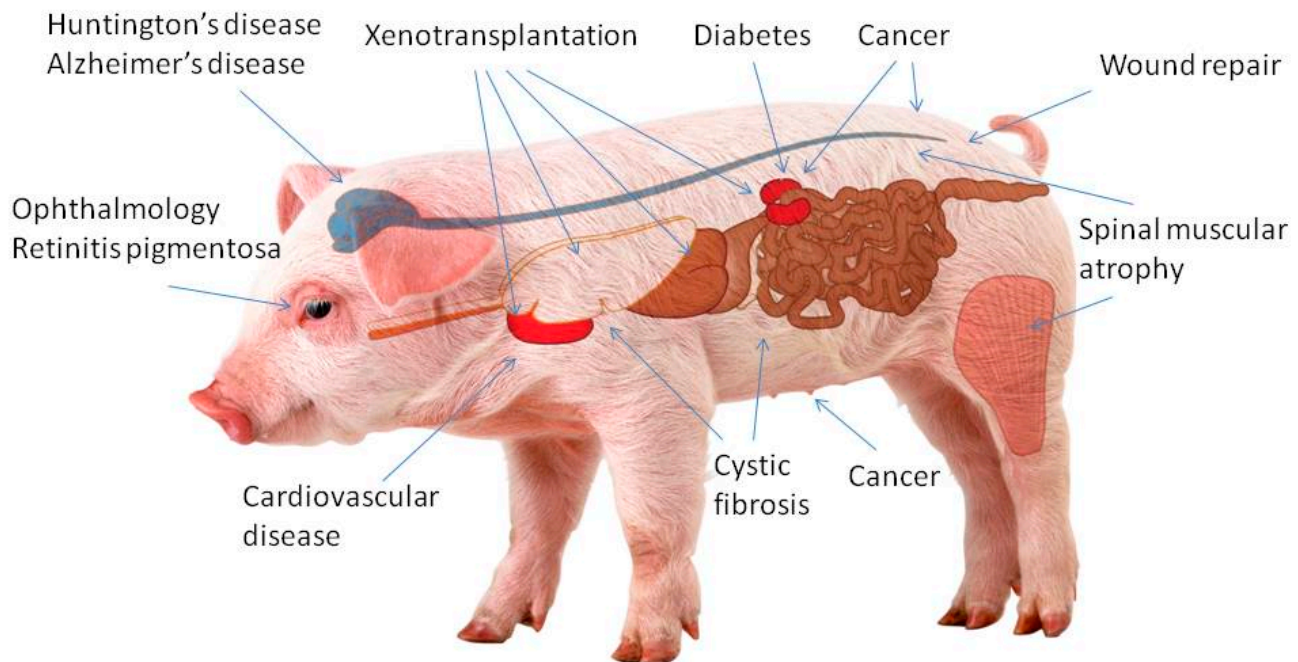

Figure 1. Swine became a model organism for biomedical research due to its similarity to humans. Pigs are ideal organisms for studying human health and disease. Their genome is three times closer than the mouse genome to that of humans.

The efficiency of the SCNT method in swine models varies from 0.2% to 7% of new-borns per constructed embryo [7,9,19]. The low success rate limits the extensive application of the pig SCNT technique in biomedical research or agricultural purposes [20]. The SCNT method uses somatic cells with low viability and not fully reprogrammed epigenetic memory. This causes swine models to develop malformations (i.e., underweight, cardiac dysfunctions, and immunological dysfunctions) [21–23]. Due to the high prevalence of these abnormalities, epigenetic disorders are believed to cause mentioned symptoms during embryo development rather than genetics.

DNA methylation is an essential element in the epigenetic regulation of embryonic development, and it occurs at most CpG dinucleotides in the mammalian genome [19,24,25]. Long-term selection and adaption towards high prolificacy and meat production have transformed porcine epigenetics [26], along with associated genotypic and phenotypic changes [2,27] resulting from the modification of the epigenetic regulation of chromatin structure and transcriptional activity. During the transformation process, the porcine DNA methylome displays variable patterns in different breeds and sexes of pigs and variations in other anatomic tissues [26,28]. Here, we analysed the pig methylome of adipose tissue mesenchymal stem cell lines displaying high and low efficiency for live-born piglets in somatic cell nuclear transfer using the RRBS method.

2. Material and Methods

2.1. Ethical Approval

All animal experiments were approved by the Government of Upper Bavaria (permit number 55.2-1-54-2532-6-13) and performed according to the German Animal Welfare Act and European Union Normative for Care and Use of Experimental Animals.

2.2. Cell Lines

Mesenchymal stem cells (MSC)s lines were isolated from male pigs (n = 10 per experimental group) according to standard isolation protocol. Cells were maintained in DMEM supplemented with 10% fetal bovine serum (FBS), 100 U/mL of penicillin, and 100 mg/mL of streptomycin (Invitrogen) at 37 °C and 5% CO_2. The HCT116 DNMT1(2/2) DNMT3b (2/2) double knockout clone number 2 (DKO) cell line was a kind gift from Dr Steve Baylin. The cell line was grown in McCoys'5A medium with 10% FBS, 0.2 mg/mL Neomycin, and 0.1 mg/mL. Genomic DNA was extracted using standard phenol: chloroform extraction followed by ethanol precipitation. Cell lines descriptions are shown in Supplementary Materials Table S1.

2.3. Reduced Representation Bisulfite Sequencing (RRBS)

2.3.1. Restriction Enzyme Digestion

Three micrograms (μg) of high molecular weight genomic DNA were used for RRBS sample preparation. Each DNA sample was subjected to MspI restriction enzyme digestion. A total volume of 50 μL was used in the procedure, including 3 μL of MspI restriction enzyme (New England Biolabs, Ipswich, MA, USA) and 5 μL of MspI reaction buffer (New England Biolabs). If the total volume was lower than 50 μL, the difference was made up with nuclease-free water as recommended by the manufacturer. Incubation was performed in the thermocycler (Thermofisher, Waltham, MA, USA) at 37 °C for 15 min. Next, the DNA purification procedure was performed using AmpureXp magnetic beads (Beckman Coulter, Brea, CA, USA).

2.3.2. End Repair

The DNA fragments with 5′-CG-3′ overhangs generated by the restriction enzyme digestion were end-repaired using Nextflex Bisulfite Kit (Biooscientific, Austin, TX, USA).

2.3.3. Size Selection, Adenylation, and Adapter Ligation

After end-repair, the SPRI double-size selection method combined with DNA purification was applied using AmpureXp magnetic beads (Beckman Coulter). The Nextflex double size selection standard protocol was followed to select fragments between 200 and 300 bp (without adapters) with a mean length of around 250 bp. A total volume of 20.5 μL of preselected DNA was collected, and adenylation reactions were performed using an adenylation mix, followed by incubation in the Thermocycler (Thermofisher) at 37 °C for 30 min. A different non-diluted adapter from Nextflex Bisulfite Barcodes Kit (Bioscientific) with a unique index sequence was chosen for each sample. Adapters were not diluted according to the manufacturer's instructions. Ligation was performed for 15 min at 22 °C. Subsequently, a DNA purification procedure was performed using AmpureXp magnetic beads (Beckman Coulter).

2.3.4. Bisulfite Conversion and Amplification

The PCR products were purified using AmpureXp magnetic beads (Beckman Coulter) according to the Nextflex procedure. The purified fragments were then subjected to bisulfite conversion using the EZ DNA Methylation-Gold Kit (Zymo Research, Irvine, CA, USA). The converted DNA was PCR amplified with some modifications. PCR reaction total volume was equal to 50 μL, including 18 μL of converted DNA, 22.75 μL of nuclease-free water, 2 μL of Nextflex primer mix from Nextflex Bisulfite Barcodes Kit (Bioscientific), 1.25 μL of 10 nM dNTP Mix (ThermoScientific), and 5 μL of 1X Turbo Cx buffer (Agilent Technologies, Santa Clara, CA, USA) and 2.5 U Pfu Turbo Cx polymerase (Agilent). The thermocycling conditions: 2 min at 95 °C and 12–18 cycles of 30 s at 95 °C, 30 s at 65 °C, and 45 s at 72 °C, followed by a 7-min final extension at 72 °C.

2.3.5. Library Validation and Sequencing

The DNA libraries were quantified using the Qubit instrument (Life Technologies, Carlsbad, CA, USA) and qualified using Agilent 2100 Bioanalyzer High Sensitivity chips (Agilent Technologies). According to the manufacturer's instructions, paired-end sequencing (2 × 100 bp) was performed on the Illumina HiSeq1500.

2.4. Bioinformatics

Paired-end reads obtained from the Illumina 1500 sequencer were filtered to remove the adapter contamination, and low-quality reads were obtained using the TrimGalore! Version 0.4.0 [29]. Filtered reads were mapped to the reference genome (susScr3 version) using Bismark [30]. Per CpG, methylation statistics were extracted using an application developed at the Department of Medical Genetics, Medical University of Warsaw. Positions with SNPs, changing CpG places to CpH or TpG, were also detected and filtered using the above application. The sequences obtained in the current study were deposited in the NCBI BioProject database [31].

2.4.1. RRBS Data Analysis

Methylation levels of cytosines were analysed by methylKit.53 [32]. Briefly, the number of methylated and unmethylated CpG and non-CpG (CHG and CHH, H representing A/C/T) sites were counted for each region. CGIs were defined as regions >200 bp with a GC fraction >0.5 and an observed-to-expected ratio of CpG > 0.6. CGI shores were defined as regions 2 kb in length adjacent to CGIs. To annotate porcine CGIs, reference genome (susScr3) and annotation were downloaded from USCSand and the Ensembl, respectively. To define the differentially methylated cytosines (DMCs), multiple pairwise comparisons were performed against CpG methylation information of twenty samples and filtered (q < 0.01) using methylKit.53.

2.4.2. Mapping

S.scrofa 10.2.79 and associated GTF files were downloaded from Ensembl. The fasta sequences were prepared for bismark (v0.14.3) [33] and then mapped using bowtie 1 as recommended for bismark software. To allow compatibility with bismark and methylkit, only somatic chromosomes were retained.

2.4.3. Raw_Reads and Trimming

Raw reads were trimmed using TrimGalore! [29] with the following parameters –trim1 –phred33 –length 50 –retain_unpaired –paired. Trimmed reads were mapped to the converted pig genome using the bismark command bismark_v0.14.3/bismark –gzip -n 1 -1 pair1.fq.gz -2 pair2.fq.gz

2.4.4. Identification of Differentially Methylated Regions (DMRs)

MethylKit (https://code.google.com/p/methylkit/, accessed on 15 July 2022) was used to identify differentially methylated regions (DMRs) (bases and tiles), which show statistically significant differential methylation between two groups: high and low-efficiency AMSCs.

2.4.5. Annotation of Genomic Regions

The high-density CpG promoter (HCP), intermediate-density CpG promoter (ICP), and low-density CpG promoter (LCP) annotations were defined based on the transcription start sites (TSS) of known RefSeq genes. In detail, HCP, which indicated the "CpG-rich" promoters, was identified as having a GC density ≥0.55 and the observed to expected CpG ratio (CpG O/E) ≥ 0.6; promoters with CpG O/E # 0.4 were classified as LCP; and the remaining nonoverlapping promoter populations (0.4 < CpG O/E < 0.6) were classified as ICP. The annotated repeat elements, such as LINEs, SINEs, and LTRs, were downloaded directly from the RepeatMasker track of the UCSC Genome Browser. Other regions, such as

CGIs, exons, and introns, were downloaded from the UCSC Genome Browser. Intragenic regions were included from the TSS to the transcription termination sites (TTS), whereas the intergenic regions were defined as the complement of the intragenic regions.

3. Results

3.1. Genomic Location of Differentially Methylated Sites

We mapped the global DNA methylation patterns of adult male ADMSCs showing high and low efficiency of SCNT in pigs. We identified 3704 bases with statistically significant differences in methylation (Supplementary Table S2); 890 bases within 5 kb of a known transcript (Supplementary Table S3); 10,062 tiles with statistically significant differences in methylation (Supplementary Table S4); and 4965 tiles within 5 kb of a known transcript (Supplementary Table S5). The majority of differentially methylated sites were intergenic Figure 2, and 37% are located in known CpG islands, Figure 3.
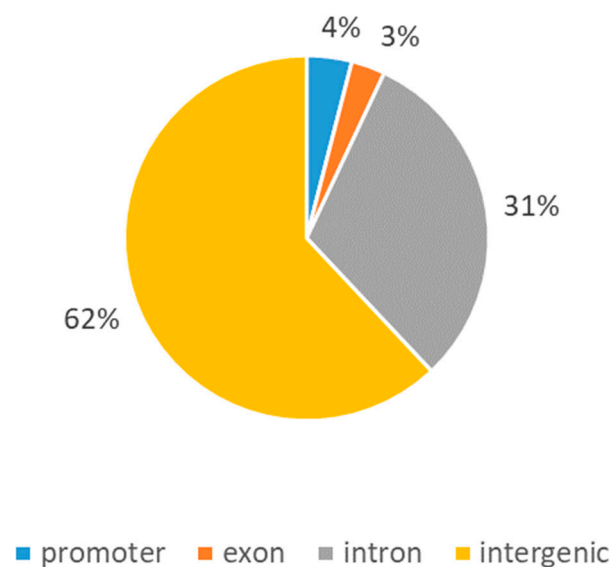

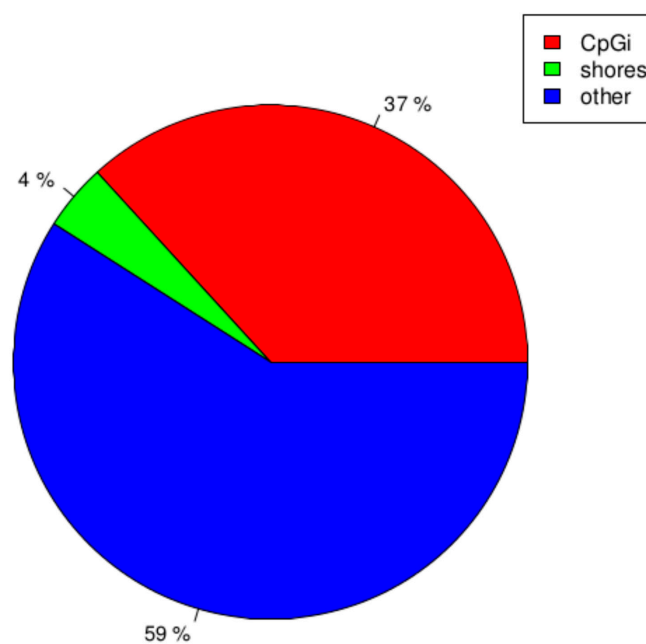**Figure 2.** Differential methylation annotations of CpG.

Figure 3. Location of differentially methylated sites.

3.2. Non-CG Methylation: CHH, CHG

Fewer differentially methylated sites were seen in other contexts: CHH 128 bases with statistically significant differences in methylation, 39 bases within 5 kb of a known transcript, 2458 tiles with statistically significant differences in methylation, and 1354 tiles within 5 kb of a known transcript (Supplementary Tables S6–S9).

In the CHG context, we identified 59 bases with statistically significant differences in methylation, 23 bases within 5 kb of a known transcript, 2554 tiles with statistically significant differences in methylation, and 1356 tiles within 5 kb of a known transcript (Supplementary Tables S10–S13).

3.3. Genome-Wide CpG Methylation and Density Patterns in Relation to Genomic Features

Unsupervised hierarchical clustering of the individual methylation profiles of high and low-efficient cells revealed separated sample groups (Figure 4). Thus, hierarchical clustering indicates that highly efficient and low efficient cells differ in methylation profiles.
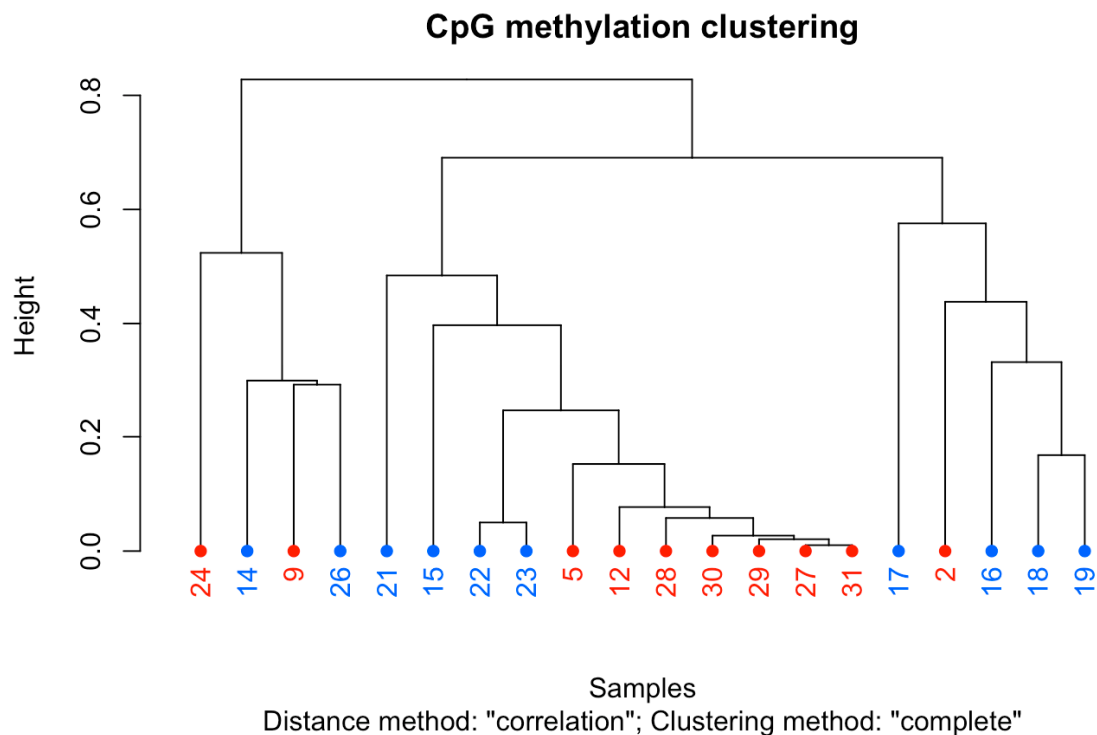

Figure 4. Hierarchical cluster analysis according to methylation patterns across analysed samples. Blue colour—low cloning efficiency cells; red colour—high cloning efficiency cells. Dendrograms were produced using correlation distance and ward clustering methods. Numbers represent the individual sample ID.

4. Discussion

Cloning has become a powerful tool for analysing gene functions, genomic imprinting, genomic re-programming, development, neurodegenerative diseases, gene therapy, and more [34–36]. Somatic cell nuclear transfer is an essential cloning tool for biomedical and epigenetic research [37]. This method enables significant development in biomedicine and disease modeling, where genome-edited mammals can be bred and used for disease research, transplantation, or to protect endangered species [5,38–41].

Due to its similarity to humans, somatic cell nuclear transfer (SCNT) and precise genome editing to generate transgenic pigs carrying the required disease phenotype may be applied to swine [6,7]. Here, we showed that according to methylation patterns, there is a clear definition of groups with low and high cloning efficiency [42–44].

DNA methylation in a promoter usually correlates with the repression [45]. Methylated genes are known to be linked with genomic region-specific DNA methylation patterns [46,47].

We investigated promoter, exon, and intron regions along the porcine genome and localised CpG islands to these genic features. Most differentially methylated sites were intergenic (Figure 2), and 37% were located in previously described CpG islands. We showed that methylation levels of CpG islands were lower than CpG island shores in the promoter, exon, and intron regions. These results demonstrated that CpG islands located in different genic features displayed effects on the methylation patterns of the associated genes. A strong relation between methylations in CpG island shores located within 2 kb of an annotated transcription start site (TSS) and the expression of related genes was reported by Irizarry and others [48]. CpG islands in exon regions showed different methylation levels than those in intron regions, suggesting that exons may affect the methylation patterns of CpG islands [49,50].

Completing the swine reference genome sequence [41,42] provides a great ability to perform porcine studies for human diseases and disorders and opens the door for targeted approaches to produce models for diseases [51–53]. Our results provide novel information for future studies of porcine epigenomics. The results based on RRBS are a powerful technology for epigenetic profiling of cell populations relevant to developmental biology and genetic engineering for porcine disease models. Further studies are necessary to investigate the similarities in methylation levels between humans and pigs for specific genomic regions. This knowledge will give us a chance to analyse disease progression, the differences observed in intron and exon methylation patterns between pig tissues and human cell lines, and the proposed adaptive evolutionary role of CpG methylation.

Recent advances in single-cell multi-omics data have shed light on the complexity of epigenetic regulation and the potential for using this information to understand the mechanisms underlying the epigenetic reprogramming process [54]. As a result, this information may be used to design more effective and efficient strategies for reprogramming the donor nucleus in SCNT. The study by Hu et al. (2018) highlights the importance of single-cell multi-omics data in exploring the molecular mechanisms underlying epigenetic reprogramming and suggests that this information could be valuable in the development of new techniques for SCNT in the future [55].

In conclusion, new perspectives in SCNT and the use of single-cell multi-omics data as a tool for understanding the mechanisms of epigenetic regulation offer novel possibilities for the future of epigenetic research. These developments have the potential to contribute to the advancement of our understanding of the biological processes underlying the epigenetic reprogramming process and the development of new techniques for SCNT applications for pig model production and contribute to the studies of human disease, xenotransplantation, and molecular breeding in agriculture.

Author Contributions: The study was conceived and designed by M.G. and P.L. Samples were maintained by P.L. Laboratory work: P.L., M.G., M.D., R.P. and K.F. Data handling—M.G. Statistical analysis was carried by T.G., K.F., P.G. and R.D.E. The manuscript was written by M.G., M.D., K.F., T.G. M.G. and M.D. revised the manuscript. Project administration—M.G. and P.L. Funding acquisition—M.G. and P.L. All authors have read and agreed to the published version of the manuscript.

References

1. Arends, M.J.; White, E.S.; Whitelaw, C.B.A. Animal and cellular models of human disease. *J. Pathol.* **2016**, *238*, 137–140. [CrossRef] [PubMed]
2. Groenen, M.A.M.; Archibald, A.L.; Uenishi, H.; Tuggle, C.K.; Takeuchi, Y.; Rothschild, M.F.; Rogel-Gaillard, C.; Park, C.; Milan, D.; Megens, H.-J.; et al. Analyses of pig genomes provide insight into porcine demography and evolution. *Nature* **2012**, *491*, 393–398. [CrossRef] [PubMed]
3. Walters, E.M.; Wells, K.D.; Bryda, E.C.; Schommer, S.; Prather, R.S. Swine models, genomic tools and services to enhance our understanding of human health and diseases. *Lab. Anim.* **2017**, *46*, 167–172. [CrossRef] [PubMed]
4. Schachtschneider, K.M.; Schook, L.B.; Meudt, J.J.; Shanmuganayagam, D.; Zoller, J.A.; Haghani, A.; Li, C.Z.; Zhang, J.; Yang, A.; Raj, K.; et al. Epigenetic clock and DNA methylation analysis of porcine models of aging and obesity. *GeroScience* **2021**, *43*, 2467–2483. [CrossRef] [PubMed]
5. Grzybek, M.; Golonko, A.; Walczak, M.; Lisowski, P. Epigenetics of cell fate reprogramming and its implications for neurological disorders modelling. *Neurobiol. Dis.* **2017**, *99*, 84–120. [CrossRef]
6. Wilmut, I.; Beaujean, N.; de Sousa, P.A.; Dinnyes, A.; King, T.J.; Paterson, L.A.; Wells, D.N.; Young, L.E. Somatic cell nuclear transfer. *Nature* **2002**, *419*, 583–586. [CrossRef]
7. Yang, X.; Smith, S.L.; Tian, X.C.; Lewin, H.A.; Renard, J.-P.; Wakayama, T. Nuclear reprogramming of cloned embryos and its implications for therapeutic cloning. *Nat. Genet.* **2007**, *39*, 295–302. [CrossRef]
8. Rideout, W.M.; Eggan, K.; Jaenisch, R. Nuclear cloning and epigenetic reprogramming of the genome. *Science* **2001**, *293*, 1093–1098. [CrossRef]
9. Zhao, J.; Whyte, J.; Prather, R.S. Effect of epigenetic regulation during swine embryogenesis and on cloning by nuclear transfer. *Cell Tissue Res.* **2010**, *341*, 13–21. [CrossRef]
10. Bendixen, E.; Danielsen, M.; Larsen, K.; Bendixen, C. Advances in porcine genomics and proteomicsc-a toolbox for developing the pig as a model organism for molecular biomedical research. *Brief. Funct. Genom. Proteom.* **2010**, *9*, 208–219. [CrossRef]
11. Flisikowska, T.; Kind, A.; Schnieke, A. The new pig on the block: Modelling cancer in pigs. *Transgenic Res.* **2013**, *22*, 673–680. [CrossRef]
12. Walters, E.M.; Prather, R.S. Advancing swine models for human health and diseases. *Mo. Med.* **2013**, *110*, 212–215.
13. Onishi, A.; Iwamoto, M.; Akita, T.; Mikawa, S.; Takeda, K.; Awata, T.; Hanada, H.; Perry, A.C. Pig cloning by microinjection of fetal fibroblast nuclei. *Science* **2000**, *289*, 1188–1190. [CrossRef]
14. Polejaeva, I.A.; Chen, S.H.; Vaught, T.D.; Page, R.L.; Mullins, J.; Ball, S.; Dai, Y.; Boone, J.; Walker, S.; Ayares, D.L.; et al. Cloned pigs produced by nuclear transfer from adult somatic cells. *Nature* **2000**, *407*, 86–90. [CrossRef]
15. Betthauser, J.; Forsberg, E.; Augenstein, M.; Childs, L.; Eilertsen, K.; Enos, J.; Forsythe, T.; Golueke, P.; Jurgella, G.; Koppang, R.; et al. Production of cloned pigs from in vitro systems. *Nat. Biotechnol.* **2000**, *18*, 1055–1059. [CrossRef]
16. Lai, L.; Prather, R.S. Creating genetically modified pigs by using nuclear transfer. *Reprod. Biol. Endocrinol.* **2003**, *1*, 82. [CrossRef]
17. Lai, L.; Kolber-Simonds, D.; Park, K.-W.; Cheong, H.-T.; Greenstein, J.L.; Im, G.-S.; Samuel, M.; Bonk, A.; Rieke, A.; Day, B.N.; et al. Production of alpha-1,3-galactosyltransferase knockout pigs by nuclear transfer cloning. *Science* **2002**, *295*, 1089–1092. [CrossRef]
18. Li, R.; Lai, L.; Wax, D.; Hao, Y.; Murphy, C.N.; Rieke, A.; Samuel, M.; Linville, M.L.; Korte, S.W.; Evans, R.W.; et al. Cloned transgenic swine via in vitro production and cryopreservation. *Biol. Reprod.* **2006**, *75*, 226–230. [CrossRef]
19. Fulka, J.; Fulka, H. Somatic cell nuclear transfer (SCNT) in mammals: The cytoplast and its reprogramming activities. *Adv. Exp. Med. Biol.* **2007**, *591*, 93–102.
20. Kurome, M.; Geistlinger, L.; Kessler, B.; Zakhartchenko, V.; Klymiuk, N.; Wuensch, A.; Richter, A.; Baehr, A.; Kraehe, K.; Burkhardt, K.; et al. Factors influencing the efficiency of generating genetically engineered pigs by nuclear transfer: Multi-factorial analysis of a large data set. *BMC Biotechnol.* **2013**, *13*, 43. [CrossRef]

21. Swindle, M.M. Swine as Surgical Models in Biomedical Research. In Proceedings of the 2009 ACVP/ASVCP Annual Meetings, Monterey, CA, USA, 5–9 December 2009; p. 4.
22. Amiridze, N.S.; Darwish, R.; Griffith, G.M.; Zoarskia, G.H. Treatment of arteriovenous malformations with hydrocoils in a Swine model. *Interv. Neuroradiol.* **2008**, *14*, 165–171. [CrossRef] [PubMed]
23. Swindle, M.M.; Makin, A.; Herron, A.J.; Clubb, F.J.; Frazier, K.S. Swine as Models in Biomedical Research and Toxicology Testing. *Vet. Pathol.* **2012**, *49*, 344–356. [CrossRef] [PubMed]
24. Bird, A. DNA methylation patterns and epigenetic memory. *Genes Dev.* **2002**, *16*, 6–21. [CrossRef] [PubMed]
25. Suzuki, M.M.; Bird, A. DNA methylation landscapes: Provocative insights from epigenomics. *Nat. Rev. Genet.* **2008**, *9*, 465–476. [CrossRef]
26. Li, M.; Wu, H.; Luo, Z.; Xia, Y.; Guan, J.; Wang, T.; Gu, Y.; Chen, L.; Zhang, K.; Ma, J.; et al. An atlas of DNA methylomes in porcine adipose and muscle tissues. *Nat. Commun.* **2012**, *3*, 850. [CrossRef]
27. Li, M.; Tian, S.; Jin, L.; Zhou, G.; Li, Y.; Zhang, Y.; Wang, T.; Yeung, C.K.; Chen, L.; Ma, J.; et al. Genomic analyses identify distinct patterns of selection in domesticated pigs and Tibetan wild boars. *Nat. Genet.* **2013**, *45*, 1431–1438. [CrossRef]
28. Wang, X.; Kadarmideen, H.N. An Epigenome-Wide DNA Methylation Map of Testis in Pigs for Study of Complex Traits. *Front. Genet.* **2019**, *10*, 405. [CrossRef]
29. Bioinformatics, B. Trim Galore! Available online: https://www.bioinformatics.babraham.ac.uk/projects/trim_galore/ (accessed on 12 March 2022).
30. Krueger, F.; Andrews, S.R. Bismark: A flexible aligner and methylation caller for Bisulfite-Seq applications. *Bioinformatics* **2011**, *27*, 1571–1572. [CrossRef]
31. National Center for Biotechnology Information NCBI BioProject. Available online: https://www.ncbi.nlm.nih.gov/bioproject/ (accessed on 9 March 2022).
32. Akalin, A.; Kormaksson, M.; Li, S.; Garrett-Bakelman, F.E.; Figueroa, M.E.; Melnick, A.; Mason, C.E. methylKit: A comprehensive R package for the analysis of genome-wide DNA methylation profiles. *Genome Biol.* **2012**, *13*, R87. [CrossRef]
33. Bioinformatics, B. Bismark. Available online: https://www.bioinformatics.babraham.ac.uk/projects/bismark/ (accessed on 27 May 2022).
34. Capecchi, M.R. How close are we to implementing gene targeting in animals other than the mouse? *Proc. Natl. Acad. Sci. USA* **2000**, *97*, 956–957. [CrossRef]
35. Matoba, S.; Zhang, Y. Somatic Cell Nuclear Transfer Reprogramming: Mechanisms and Applications. *Cell Stem Cell* **2018**, *23*, 471–485. [CrossRef]
36. Perrera, V.; Martello, G. How Does Reprogramming to Pluripotency Affect Genomic Imprinting? *Front. Cell Dev. Biol.* **2019**, *7*, 76. [CrossRef]
37. Srirattana, K.; Kaneda, M.; Parnpai, R. Strategies to Improve the Efficiency of Somatic Cell Nuclear Transfer. *Int. J. Mol. Sci.* **2022**, *23*, 1969. [CrossRef]
38. Liu, X.; Chen, L.; Wang, T.; Zhou, J.; Li, Z.; Bu, G.; Zhang, J.; Yin, S.; Wu, D.; Dou, C.; et al. TDG is a pig-specific epigenetic regulator with insensitivity to H3K9 and H3K27 demethylation in nuclear transfer embryos. *Stem Cell Rep.* **2021**, *16*, 2674–2689. [CrossRef]
39. Yue, Y.; Xu, W.; Kan, Y.; Zhao, H.-Y.; Zhou, Y.; Song, X.; Wu, J.; Xiong, J.; Goswami, D.; Yang, M.; et al. Extensive germline genome engineering in pigs. *Nat. Biomed. Eng.* **2021**, *5*, 134–143. [CrossRef]
40. Tian, X.C.; Kubota, C.; Enright, B.; Yang, X. Cloning animals by somatic cell nuclear transfer–biological factors. *Reprod. Biol. Endocrinol.* **2003**, *1*, 98. [CrossRef]
41. Fatira, E.; Havelka, M.; Labbé, C.; Depincé, A.; Iegorova, V.; Pšenička, M.; Saito, T. Application of interspecific Somatic Cell Nuclear Transfer (iSCNT) in sturgeons and an unexpectedly produced gynogenetic sterlet with homozygous quadruple haploid. *Sci. Rep.* **2018**, *8*, 5997. [CrossRef]
42. Schachtschneider, K.M.; Madsen, O.; Park, C.; Rund, L.A.; Groenen, M.A.M.; Schook, L.B. Adult porcine genome-wide DNA methylation patterns support pigs as a biomedical model. *BMC Genom.* **2015**, *16*, 743. [CrossRef]
43. Ziller, M.J.; Müller, F.; Liao, J.; Zhang, Y.; Gu, H.; Bock, C.; Boyle, P.; Epstein, C.B.; Bernstein, B.E.; Lengauer, T.; et al. Genomic Distribution and Inter-Sample Variation of Non-CpG Methylation across Human Cell Types. *PLoS Genet.* **2011**, *7*, e1002389. [CrossRef]
44. Shirane, K.; Toh, H.; Kobayashi, H.; Miura, F.; Chiba, H.; Ito, T.; Kono, T.; Sasaki, H. Mouse Oocyte Methylomes at Base Resolution Reveal Genome-Wide Accumulation of Non-CpG Methylation and Role of DNA Methyltransferases. *PLoS Genet.* **2013**, *9*, e1003439. [CrossRef]
45. Baribault, C.; Ehrlich, K.C.; Ponnaluri, V.K.C.; Pradhan, S.; Lacey, M.; Ehrlich, M. Developmentally linked human DNA hypermethylation is associated with down-modulation, repression, and upregulation of transcription. *Epigenetics* **2018**, *13*, 275–289. [CrossRef] [PubMed]
46. Raza, M.A.; Yu, N.; Wang, D.; Cao, L.; Gan, S.; Chen, L. Differential DNA methylation and gene expression in reciprocal hybrids between Solanum lycopersicum and S. pimpinellifolium. *DNA Res.* **2017**, *24*, 597–607. [CrossRef] [PubMed]
47. Bell, J.T.; Pai, A.A.; Pickrell, J.K.; Gaffney, D.J.; Pique-Regi, R.; Degner, J.F.; Gilad, Y.; Pritchard, J.K. DNA methylation patterns associate with genetic and gene expression variation in HapMap cell lines. *Genome Biol.* **2011**, *12*, R10. [CrossRef] [PubMed]
48. Irizarry, R.A.; Ladd-Acosta, C.; Wen, B.; Wu, Z.; Montano, C.; Onyango, P.; Cui, H.; Gabo, K.; Rongione, M.; Webster, M.; et al. The human colon cancer methylome shows similar hypo- and hypermethylation at conserved tissue-specific CpG island shores. *Nat. Genet.* **2009**, *41*, 178–186. [CrossRef] [PubMed]

49. Chen, X.; Shen, L.-H.; Gui, L.-X.; Yang, F.; Li, J.; Cao, S.-Z.; Zuo, Z.-C.; Ma, X.-P.; Deng, J.-L.; Ren, Z.-H.; et al. Genome-wide DNA methylation profile of prepubertal porcine testis. *Reprod. Fertil. Dev.* **2018**, *30*, 349. [CrossRef]
50. Yuan, X.-L.; Gao, N.; Xing, Y.; Zhang, H.-B.; Zhang, A.-L.; Liu, J.; He, J.-L.; Xu, Y.; Lin, W.-M.; Chen, Z.-M.; et al. Profiling the genome-wide DNA methylation pattern of porcine ovaries using reduced representation bisulfite sequencing. *Sci. Rep.* **2016**, *6*, 22138. [CrossRef]
51. Prather, R.S.; Walters, E.M.; Wells, K.D. Swine in Biomedical Research 2014. *Lab Anim.* **2015**, *44*, 9. [CrossRef]
52. Lunney, J.K.; Van Goor, A.; Walker, K.E.; Hailstock, T.; Franklin, J.; Dai, C. Importance of the pig as a human biomedical model. *Sci. Transl. Med.* **2021**, *13*, eabd5758. [CrossRef]
53. Gutierrez, K.; Dicks, N.; Glanzner, W.G.; Agellon, L.B.; Bordignon, V. Efficacy of the porcine species in biomedical research. *Front. Genet.* **2015**, *6*, 293. [CrossRef]
54. Lee, J.; Hyeon, D.Y.; Hwang, D. Single-cell multiomics: Technologies and data analysis methods. *Exp. Mol. Med.* **2020**, *52*, 1428–1442. [CrossRef]
55. Hu, Y.; An, Q.; Sheu, K.; Trejo, B.; Fan, S.; Guo, Y. Single Cell Multi-Omics Technology: Methodology and Application. *Front. Cell Dev. Biol.* **2018**, *6*, 28. [CrossRef]